Hindawi Publishing Corporation
Journal of Geochemistry
Volume 2014, Article ID 168938, 10 pages
http://dx.doi.org/10.1155/2014/168938

Research Article

Lead Immobilization and Hydroxamate Ligand Promoted Chloropyromorphite Dissolution

Nadia K. Adam[1,2,3]

[1] *Department of Environmental Engineering and Geological Sciences, Fitzpatrick, University of Notre Dame, South Bend, IN 27695-7619, USA*
[2] *Department of Geology & Geophysics, University of Wyoming, Laramie, WY 82071, USA*
[3] *Biomineral Systems LLC, South Bend, IN 27695, USA*

Correspondence should be addressed to Nadia K. Adam; nadia.k.adam@gmail.com

Received 2 February 2014; Revised 29 May 2014; Accepted 29 May 2014; Published 20 July 2014

Academic Editor: Andrew Hursthouse

The immobilization of lead, a major environmental contaminant, through phosphate amendments to form the sparingly soluble lead phosphate mineral chloropyromorphite [$Pb_5(PO_4)_3$] (CPY) is an effective *in situ* strategy for soil remediation. An important question is the effect of microbial processes on this remediation. Here, we investigate the role of the microbial siderophore ligand desferrioxamine-D_1 (DFO-D_1) and its analog acetohydroxamic acid (aHA) in CPY lability using pH-dependent batch dissolution kinetics and model calculations. Both (0.01) M aHA and (0.00024) M DFO-D_1 are similarly effective and enhance lead release from CPY by more than two orders of magnitude at pH > 6 compared to in the absence of ligands. This is consistent with model calculations of pH-dependent (aqueous) complexation of lead with hydroxamate ligands. More importantly, pH-dependent ligand sorption is predictive of its ligand promoted dissolution behavior. Our results suggest that organic ligands can significantly increase CPY lability at alkaline pHs in soils and sediments and that addition of P amendments to immobilize Pb as CPY may only be successful at acid pHs.

1. Introduction

Lead is a major environmental contaminant in soils, sediments, and surface waters [1] and concentrations greater than 10 μg/dL are toxic to children. Exposure to lead contaminated soils is one of the main pathways of lead toxicity [2]. Lead immobilization through phosphate amendments to form the sparingly soluble lead phosphate mineral, chloropyromorphite [$Pb_5(PO_4)_3$] (CPY), can be an effective *in situ* strategy to remediate lead in soils [3]. The effectiveness of this strategy depends on the long-term stability of CPY, which may be affected by pH and the presence of organic ligands. Microbial organic ligands such as trihydroxamate siderophores, secreted by bacteria and fungi, are commonly present in soil environments [4, 5]. Siderophores can chelate Fe(III) with high binding affinities and also trace metals such as Pb(II) [6]. Therefore, hydroxamate siderophores such as desferrioxamine-B (DFO-B) can potentially increase the lability of CPY. For example, trihydroxamate siderophores [7] and acetohydroxamic acid containing only one hydroxamate moiety [8] have been shown to promote dissolution of a Fe-oxide mineral, goethite. It is therefore important to characterize proton-promoted and organic ligands-promoted CPY dissolution commonly present in terrestrial environments for predicting the mobility of CPY particles in porous media such as soils.

Proton-promoted CPY dissolution has been investigated as a function of pH and aging by Scheckel and Ryan [3] and more recently by Xie and Giammar [9]. Schekel and Ryan [3] show that CPY dissolves rapidly; however, their dissolution results are limited to 1 h and 24 h only. Xie and Giammar [9] show that similar to the equilibrium solubility of CPY, the rate of dissolution also decreases with increasing pH. Recent investigation of DFO-B promoted CPY dissolution by Manecki and Maurice [10] shows that DFO-B enhances Pb(II) release between pH 6 and 11 probably due to strong complexation of Pb(II) with DFO-B in this pH range. In spite of these previous investigations, the effect of ligand size and

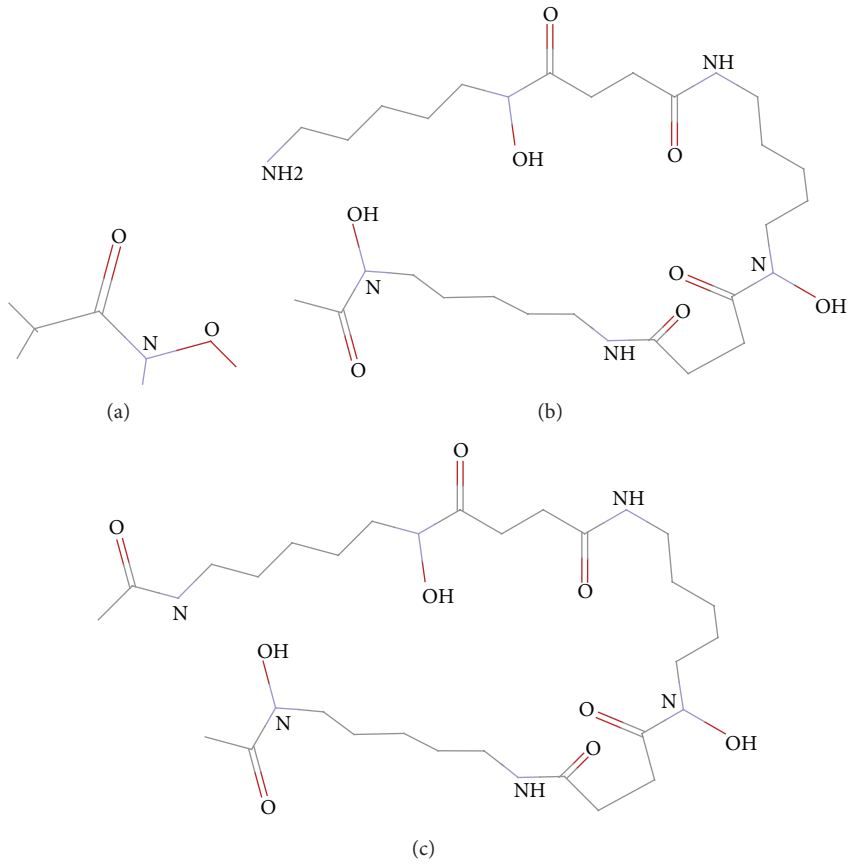

Figure 1: Molecular structures of (a) acetohydroxamic acid, (b) desferrioxamine-B, and (c) desferrioxamine-D_1.

charge on CPY dissolution is not yet properly understood. In addition, proton-promoted dissolution of CPY over longer time periods and batch dissolution kinetics of relevant soil ligands especially DFO-D_1 promoted dissolution have not been fully characterized. Here, we investigate DFO-D_1 (an acetyl derivative of DFO-B) and acetohydroxamic acid (aHA) promoted dissolution of CPY in comparison to its proton-promoted dissolution with respect to its equilibrium solubility and rate of dissolution (see Figure 1 for structural information). aHA containing a single hydroxamate moiety is representative of hydroxamate siderophores found in soils and surface waters. Results from this study provide a comparison of DFO-B (a charged trihydroxamate siderophore) (see [11]) and DFO-D_1 (an uncharged trihydroxamate siderophore) promoted CPY dissolution and also characterize the effect of ligand size and charge including stearic factors on ligand-promoted dissolution.

It is well known that, ligands (aHA and $DFOD_1$) are expected to enhance Pb(II) release upon CPY dissolution. However, the effect of pH is not known a priori because ligand promoted and proton (or hydroxyl) promoted dissolution of CPY may operate in tandem or in parallel. Generally, ligand-promoted pathways are dominant near the PZC of the mineral [8] although the contribution from proton/hydroxyl/reductive dissolution pathways to ligand-promoted pathway is not known. The PZC of CPY is estimated as 6.7 based on its isoelectric point determination. We investigated ligand-promoted dissolution of CPY at low (pH 4) and high (pH 9) pH relative to its PZC in addition to near its PZC to gain insights into the contribution from proton- or hydroxyl-promoted pathways to the ligand-promoted pathway of CPY dissolution. Proton-promoted pathways are generally dominant at very low pH, that is, between pH 2 and 3; the reductive dissolution pathway is expected to be dominant below pH 2 [8]; and the hydroxyl-promoted dissolution pathway is dominant at pH ≥ 9 [8].

The objectives of this study are (1) to investigate the proton-promoted batch dissolution kinetics at pH 2.5 and equilibrium dissolution in the absence of ligands between pHs 2 and 9 and (2) to investigate equilibrium dissolution and batch dissolution kinetics of DFO-D_1 and aHA promoted dissolution of CPY near pHs 4, 6.5, and 9. We employ one-stop batch dissolution experiments similar to Scheckel and Ryan [3] and Xie and Giammar [9] to mimic CPY dissolution in natural systems. We observed that aHA and DFO-D_1 dissolve CPY rapidly with the concentration of dissolved Pb achieving steady state within the hour. The amount of dissolved Pb(II) from CPY dissolution in the presence of 0.01 M aHA is similar to that in the presence of 0.00024 M DFO-D_1 aHA and DFO-D_1 increased CPY dissolution between pH 6 and 10 by more than two orders of magnitude.

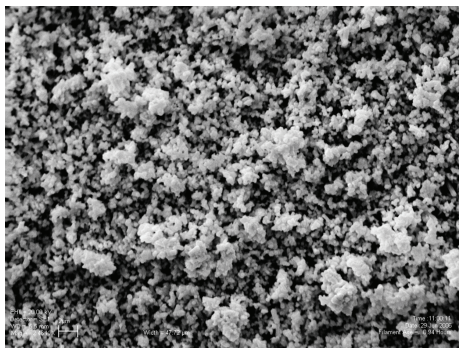

Figure 2: Scanning electron micrograph of CPY showing essentially a monodispersion of micron size cylindrical particles with some smaller particles.

2. Methods

2.1. Synthesis and Characterization of Chloropyromorphite. Chloropyromorphite (CPY) is synthesized by combining 500 mL of 0.30 M $PbNO_3$ and 0.14 M K_2HPO_4 (in 0.05 M NaCl) solutions. Two burettes are filled with $PbNO_3$ and K_2HPO_4, respectively, and allowed to empty into a 2 L polypropylene (PP) Erlenmeyer flask containing 1 L of Millipore H_2O at a rate of 24 drops per minute. A similar method is used by Manecki et al. [12] to synthesize hydroxylpyromorphite. White particles of CPY precipitate quickly upon mixing solution. Once all the 500 mL solutions of $PbNO_3$ and K_2HPO_4 have been emptied in the Erlenmeyer flask, the precipitate is aged in suspension for 24 hours. Scheckel and Ryan [3] showed that CPY aged for 24 h is as stable as CPY aged for 1 year. The CPY suspension is collected in 4, 250 mL PP bottles and washed 4 times with deionized (Millipore) water. After washing, the suspension is freeze-dried for storage. The X-ray diffraction pattern of CPY is consistent with chloropyromorphite and the EDS shows peaks for only Pb, P, O, and Cl. Figure 1 shows scanning electron microscope (SEM) micrograph of CPY. CPY consisted of hexagonal particles mostly measuring ~1 μm in diameter with some smaller particles (Figure 2). The PZC of CPY was separately determined and found to be 6.7 (data not shown).

2.1.1. Solution Preparation. Analytical grade reagents and Millipore water are used in preparation of all solutions. aHA is purchased from Sigma Aldrich and was not additionally purified. DFO-D_1 is prepared using a modified procedure of Kraemer et al. [7]. Ligand solutions are prepared fresh and stirred before each experiment.

2.2. Sorption Measurements. The aHA sorption isotherm experiments on CPY are conducted at pH 6.5 in 28 mL polycarbonate centrifuge tubes. Samples have a suspended solids concentration of 10.0 g kg^{-1}, constant ionic background of 0.01 M $NaNO_3$, and total sample mass of 25 ± 0.01 g. All aqueous solutions for sorption experiments (0.01 $NaNO_3$, 0.01 M HCl, 0.01 M NaOH, and 0.01 M aHA) are prepared using analytical grade reagents and Millipore water. aHA was added at 0.025 M concentration using a micropipette.

Table 1: Selected speciation constants used in model calculations.

Reaction	log K
(CPY) $Pb_5(PO_4)_3Cl = 5Pb^{2+} + 3PO_4^{3-} + Cl^-$	−80.85
$DFOB^{3-} + H^+ = H(DFOB)^{2-}$	10.87
$H(DFOB)^{2-} + H^+ = H_2(DFOB)^-$	9.57
$H_2(DFOB)^- + H^+ = H_3(DFOB)$	8.97
$H_3(DFOB) + H^+ = H_4(DFOB)^+$	8.35
$Pb^{2+} + H(DFOB)^{2-} = PbH(DFOB)$	10.0
$Pb^{2+} + H_2(DFOB)^- = PbH_2(DFOB)^+$	9.25
$Pb^{2+} + H_3(DFOB)^- = PbH_3(DFOB)^{2+}$	5.92
$2Pb^{2+} + H(DFOB)^{2-} = Pb_2H(DFOB)^{2+}$	16.29
$Pb^{2+} + H_2O = Pb(OH)^+ + H^+$	−7.597
$Pb(OH)_2 + 2H^+ = Pb^{2+} + 2H_2O$	−17.094
$Pb^{2+} + 3H_2O = Pb(OH)^{-3} + 3H^+$	−28.091
$2Pb^{2+} + H_2O = Pb_2(OH)^{+3} + H^+$	−6.397
$3Pb^{2+} + 4H_2O = Pb_3(OH)_4^{+2} + 4H^+$	−23.88
$4Pb^{2+} + 4H_2O = Pb_4(OH)_4^{+4} + 4H^+$	−20.888
$2H^+ + PO_4^{-3} = H_2PO_4^-$	19.573
$3H^+ + PO_4^{-3} = H_3PO_4$	21.721
$H^+ + PO_4^{-3} = HPO_4^{-2}$	12.375
$H_2O - H^+ = OH^-$	−13.997
$Pb^{+2} + PO_4^{-3} + 2H^+ = PbH_2PO_4^+$	21.073
$Pb^{+2} + PO_4^{-3} + H^+ = PbHPO_4$	15.475

Samples are equilibrated on a shaker at a moderate rate at 298 K temperature for 24 h. The aHA sorption on CPY is measured as a function of time for batch sorption kinetics using an analogous procedure as described earlier. The pH is adjusted to 4, 5.5, 6, 7, 8, 9, and 9.5 using 0.01 M HCl or 0.01 M NaOH. After equilibration, samples are filtered and the concentration of aHA is measured colorimetrically (400–650 nm) as a complex in the presence of excess Fe(III) using modified procedures of Bergmann and Segal [13] and Gillam et al. [14].

2.3. Dissolution Measurements. The DFO-D_1, aHA, or proton-promoted batch dissolution experiments are conducted in 28 mL polycarbonate centrifuge tubes at 298°K with 10 g/kg solid's concentration and 0.01 M $NaNO_3$ as background electrolyte. aHA or DFO-D_1 is added to make a final concentration of 0.01 M aHA or 0.00024 M DFO-D_1 to CPY suspension and the pH is adjusted to 4, 6.5, or 9.0 using 0.01 M HNO_3 or 0.01 M NaOH. The final mass is made to 25 g with the addition of 0.01 M $NaNO_3$ and the samples are equilibrated over 1–192 h by shaking at a moderate rate. After equilibration the samples are centrifuged at 10,000 rpm for 15 minutes and filtered using 0.2 μm polycarbonate hydrophobic filters. The supernatants are refrigerated for analysis of dissolved Pb. Dissolved total Pb was analyzed using a Perkin Elmer Optima 2000 ICP-OES instrument against Pb standards made from a standard solution of Pb (Spex Certi-prep 999 ug/g standards from Fisher Scientific) diluted with 0.01 M $NaNO_3$.

2.4. Modeling Aqueous Geochemical Speciation. Visual Minteq ver. 2.6.1 software program is used for modeling dissolved Pb speciation in supernatants from CPY

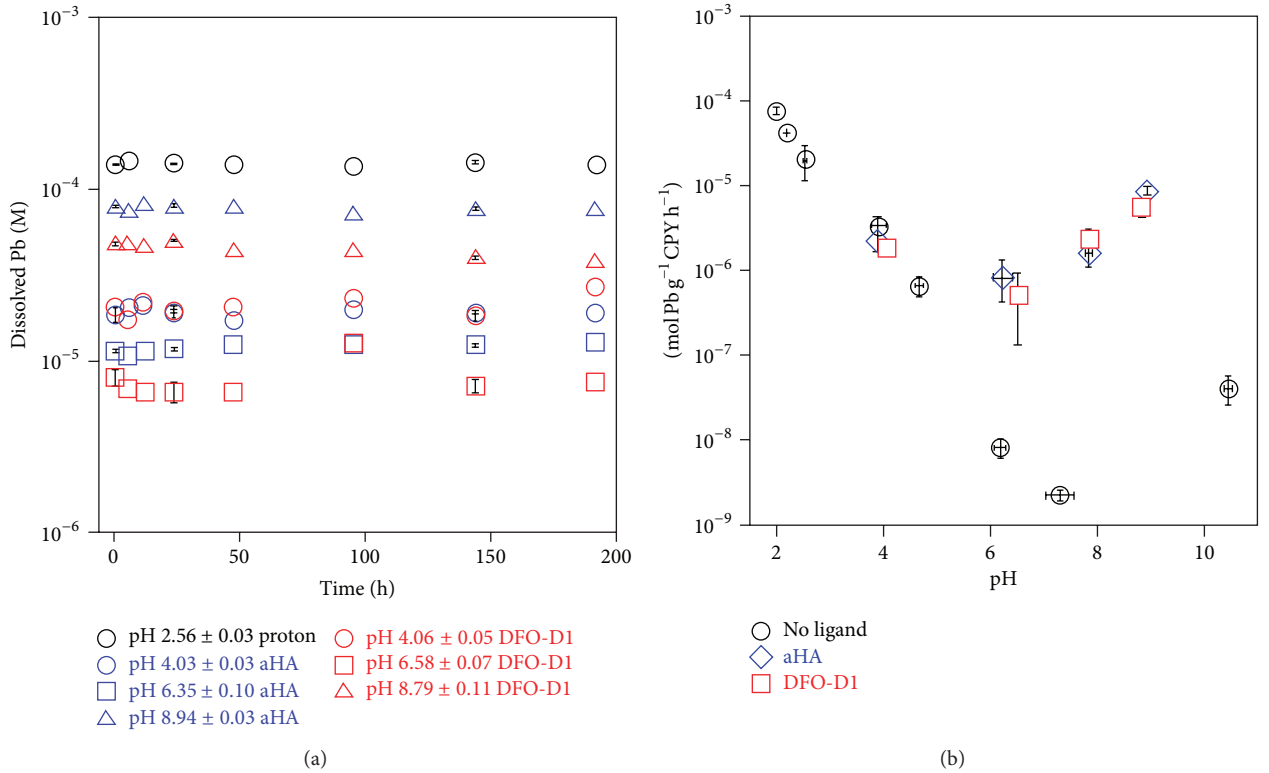

FIGURE 3: (a) Batch dissolution kinetics of CPY in the absence of ligands near pH 2.5; in the presence of DFO-D_1 and aHA near pHs 4, 6, and 9; (b) compilation of average 1 h dissolution rates of CPY in the absence and presence of ligands (aHA, DFO-D_1) plotted as a function of pH.

dissolution. All species along with their respective constants specified in the default thermodynamic database (thermo.vdb) of Visual Minteq are used (see Table 1). CPY specified as chloropyromorphite (soil) with a stability constant of −80.4 is used in all calculations. The component database (comp_2008.vda) is modified to include DFO-B and aHA components. All pertinent DFO-B and aHA species along with their reaction constants from Hepinstall et al. [15] are added to the thermodynamic database (Table 1). Ionic strength (at 0.01 M) and pH are fixed and CPY is modeled as an infinite solid phase for all calculations. Infinite solid phases are those that do not dissolve completely during equilibration and control the solution ion activities. There is no difference, however, in modeling a solid as a finite or infinite solid phase when the solid does not dissolve completely as in our (CPY) case.

3. Results and Discussion

3.1. Kinetics of CPY Dissolution. Proton-promoted dissolution of CPY at pH 2.5 over a period of 1–186 h is shown in Figure 3(a). CPY dissolves within the hour. The amount of dissolved Pb remains fairly constant between 1 and 186 h at ~$1.4*10^{-4}$ M. Our CPY shows less dissolution compared to the 1-month aged CPY of Xie and Giammar [9] probably due to lower pH (of 2) and greater concentration of smaller 10–20 nm particles in their study (Figure 3(a)).

DFO-D_1 or aHA promoted CPY dissolution near pHs 4.0, 6.5, and 9.0 over a period of 1–186 h is also shown in Figure 3(a). The ligands (DFO-D_1 or aHA) similar to protons also caused CPY to dissolve within the hour and the concentration of dissolved Pb remained essentially constant over the period of 186 hours (Figure 3(a)). Minimum CPY dissolves near its PZC of 6.7 as promoted by aHA or DFO-D_1. This is consistent with CPY dissolution near its PZC being dominated by the ligand-promoted pathway with minimal contribution from proton, hydroxyl, or reductive dissolution pathways. More CPY dissolves near pH 4 compared to near its PZC and maximum CPY dissolves near pH 9 (Figure 3(a)) probably due to contribution from the proton- and hydroxyl-promoted pathways in addition to the ligand-promoted pathway.

Figure 3(b) shows a comparison of the 1 h batch dissolution rates in the absence and presence of ligands as a function of pH. These results indicate that the rate of CPY dissolution is pH dependent (Figure 3(b)). In the absence of ligands, the rate of batch CPY dissolution decreases with increasing pH until about pH 7 (Figure 3(b)), similar to the findings of Scheckel and Ryan [3] and Xie and Giammar [9], with flow-through reactors. The rate of CPY dissolution increases near pH 10 probably due to contribution from the hydroxyl-promoted pathway (see Figure 3(b)). In the presence of aHA or DFO-D_1, the rate of CPY dissolution is greater near pH 4 or 9 than near its PZC (Figure 3(b)). Near pH 4 in the presence of ligands, the CPY dissolution rate is similar to the proton-promoted dissolution rate. However, near its PZC and pH 9, the ligand-promoted dissolution rate is much faster than the hydroxyl-promoted dissolution rate (Figure 3(b)).

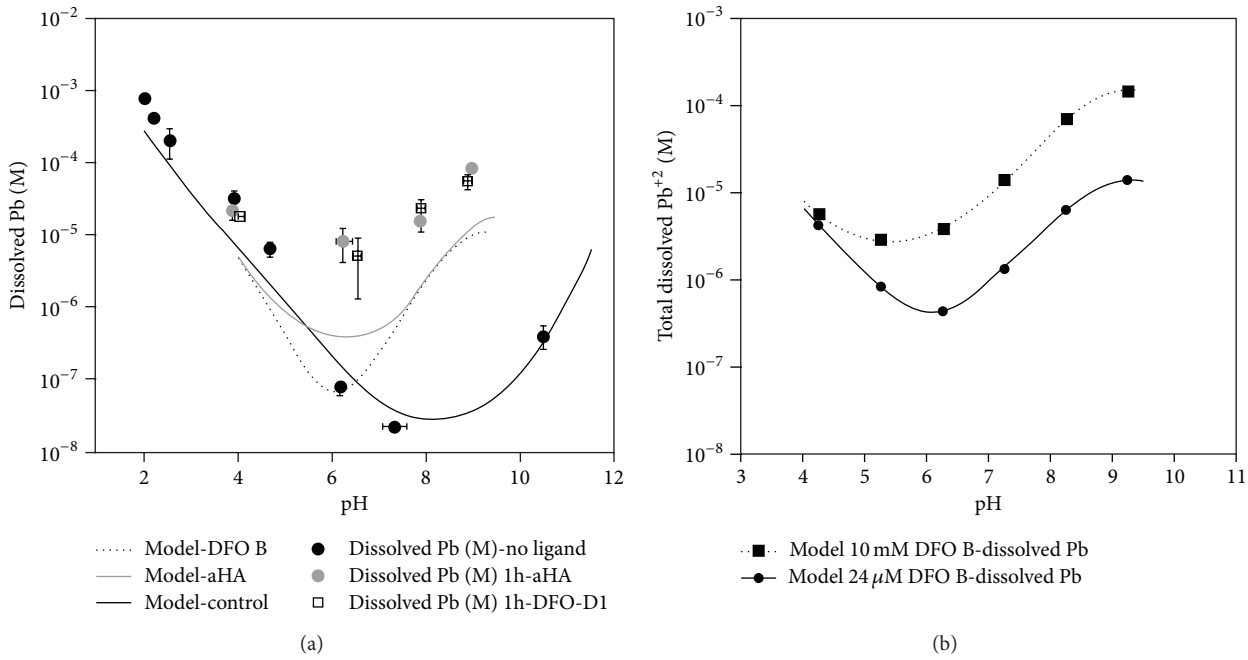

Figure 4: (a) A comparison of equilibrium aHA or DFO-D_1 promoted dissolution of CPY as a function of pH compared to equilibrium CPY dissolution in the absence of ligands along with Visual Minteqa 2.6.1 model calculations; (b) model calculations of 0.01 M DFO-B versus 0.00024 M DFO-B promoted CPY dissolution.

These results suggest that pH-dependent interactions of CPY with ligands affect the contribution of proton- and hydroxyl-promoted pathways to the ligand-promoted pathway.

3.2. Equilibrium DFO-D_1, aHA, Promoted CPY Dissolution. Figure 4(a) shows the pH-dependent trend in aHA or DFO-D_1 promoted equilibrium CPY dissolution compared to the control in the absence of ligands. Our results show that CPY dissolution as promoted by aHA or DFO-D_1 increases at pH > 6 similar to equilibrium DFO-B promoted CPY dissolution in Manecki and Maurice's study [10] (Figure 4(a)). In the absence of ligands, the concentration of dissolved Pb increases with decreasing pH between pHs 6.5 and 2.1 (Figure 4(a)). These results are consistent with the results of Scheckel and Ryan [3] and also Xie and Giammar [7] who show less CPY dissolution with increasing pH (2–6). The trend in dissolved Pb due to pH-dependent CPY dissolution (in the absence of ligands) closely matches the modeled equilibrium CPY dissolution with K_{sp} of CPY at $10^{-80.4}$ (see Figure 4(a)). This is also consistent with the results of Xie and Giammar [7], showing K_{sp} of $10^{-80.4}$ as a better fit to their results on proton-promoted CPY dissolution than the widely reported K_{sp} of $10^{-84.4}$.

To investigate our hypothesis that aHA or DFO-D_1 promoted CPY dissolution was greater at pHs 4 and 9 due to the contribution from proton- or hydroxyl-promoted pathways, we compare equilibrium dissolved Pb concentration in the absence of ligands with that in the presence of aHA or DFO-D_1 both from model calculations and trends in experimental data. We find that, at pH 4, equilibrium dissolved Pb concentration in the absence of ligands is slightly greater than equilibrium dissolved Pb concentration in the presence of aHA or DFO-D_1, suggesting that the contribution from ligand-promoted pathway is minimal near pH 4 (Figure 4(a)). Near pH 6.5 and pH 9, however, ligand-promoted CPY dissolution pathway dominates as shown by more than 2 orders of magnitude of dissolved Pb above pH 6 in the presence of aHA or DFO-D_1 than in the absence of ligands (Figure 4(a)).

The pH-dependent trend in equilibrium dissolved Pb concentration from DFO-D_1 promoted CPY dissolution is similar to that observed with aHA promoted CPY dissolution (Figure 4(a)). Surprisingly, the experimental data as shown in Figure 4(a) indicates that the efficacy of 0.00024 M trihydroxamate ligand (DFO-D_1) and 0.01 M monohydroxamate ligand (aHA) in dissolving CPY is comparable at all pHs within error. It is well known that the efficacy of the ligand-promoted dissolution pathway is directly dependent on the concentration of the sorbed complex [16–18] assuming that the adsorption sites contribute similarly to dissolution and that the structure of sorbed complex does not change with pH [8]. Given more than two orders of magnitude smaller concentration of DFO-D_1 compared to aHA and its larger mass and size (compared to aHA) causing possible stearic impediments affecting its capacity to sorb, we would expect much less dissolution in the presence of DFO-D_1 than in the presence of aHA. Since stability constants for DFO-D_1 are not available, DFO-B of similar structure, mass, and size is used as an analogue for DFO-D_1 for model calculations. The model calculations of aHA and DFO-B promoted CPY dissolution do indeed show nearly an order of magnitude less

total Pb released with DFO-B compared to aHA promoted dissolution, respectively (Figure 4(a)). However, the experimental data showed similar total dissolved Pb with DFO-D_1 or aHA promoted CPY dissolution. In addition, the model calculations of CPY dissolution in the presence of 0.00024 M DFO-B compared to 0.01 M DFO-B showed an order of magnitude increase in Pb released consistent with the expectation that amount of Pb^{2+} released from CPY dissolution should increase with increase in ligand concentration (Figure 4(b)).

This discrepancy between DFO-B model calculations and DFO-D_1 experimental data may be mainly because of two reasons. First, DFO-D_1 is in fact more effective than DFO-B in dissolving CPY and releasing Pb. Kraemer et al. [7] compare DFO-B versus DFO-D_1 promoted goethite dissolution at the same ligand concentration of 0.00024 M and show that DFO-D_1 is an order of magnitude more effective than DFO-B. In addition, CPY dissolution of Manecki and Maurice [10] shows that DFO-B enhances Pb release from CPY by approximately only an order of magnitude (compared to the control) versus 2 orders of magnitude more Pb released in the presence of DFO-D_1 in our data (Figure 4(a)). Another reason may be the difference in pH-dependent sorption behavior of aHA/DFO-D_1 in addition to the pH-dependent concentration of dissolved Pb-aHA/Pb-DFO-D_1 complexes affecting CPY dissolution. DFO-B adsorption on goethite shows cation-like behavior while DFO-D_1 shows ligand-like adsorption behavior and adsorbs twice as much on goethite compared to DFO-B [7]. Lead-ligand complexation and ligand sorption as a function of pH are investigated in more detail below by (1) modeling dissolved Pb speciation upon CPY dissolution in the absence of ligands and in the presence of aHA or DFO-B and (2) by investigating pH-dependent aHA sorption behavior on CPY.

3.3. Lead Speciation in the Liquid Phase from Model Calculations of CPY Dissolution. Figures 5(a), 5(b), and 5(c) show the amount of calculated total Pb released in the absence of ligands or in the presence of aHA or DFO-B. Figure 5(a) shows model calculations of pH-dependent Pb speciation upon CPY dissolution in the absence of ligands. Below pH 7, the total dissolved Pb is essentially a sum of Pb^{2+} and $PbCl^+$, both of which decrease steadily with increasing pH (Figure 5(a)). Above pH 7, $PbOH^+$ is the main component of the total dissolved Pb (Figure 5(a)). Figure 5(b) shows model calculations of pH-dependent Pb speciation in aHA promoted CPY dissolution. Pb forms two complexes with aHA, a positively charged $Pb(aHA)^+$ complex and a neutral $Pb(aHA)_2$ complex (see Table 1). Similar to the control, uncomplexed Pb^{2+} is one of the main species comprising total dissolved Pb at low pH (4-5) with steadily decreasing contribution with increasing pH (Figure 5(b)). However, unlike in the control, $Pb(aHA)^+$ dominates at all pHs except between pHs 4 and 5 (Figure 5(b)). At pH above 7, the neutral species $Pb(aHA)_2$ controls total Pb released with some contribution from $Pb(aHA)^+$ species (Figure 5(b)). Figure 5(c) shows model calculations of Pb speciation in DFO-B promoted CPY dissolution. Lead forms four aqueous complexes with DFO-B: HPb(DFOB), $H_2PB(DFOB)^+$, $H_3Pb(DFOB)^{2+}$, and $HPb_2(DFOB)^{2+}$ (Table 1; [15]). Unlike aHA, in DFO-B promoted CPY dissolution, un-complexed Pb as Pb^{2+} dominates Pb speciation until about pH 6 (Figure 5(c)). Above pH 6, Pb-DFO-B complexes in particular, positively charged $H_2Pb(DFOB)^+$ and to a lesser extent, HPb(DFOB) control Pb speciation in solution (Figure 5(c)). Furthermore, Pb-aHA aqueous complexes control the speciation of dissolved Pb between pHs 5 and 9 and Pb-DFO-B aqueous complexes control the speciation of dissolved Pb between pHs 6 and 9 suggesting maximum enhancement in Pb release from CPY dissolution in these pH ranges, respectively. The model aqueous speciation calculations, therefore, explain the pH-dependent trends in the experimental data showing essentially similar amounts of total Pb dissolved near pH 4 and an enhancement in Pb release from CPY dissolution in the presence of aHA or DFO-D_1 compared to the control at pH > 6 assuming that Pb-DFO-D_1 complexes are analogous to Pb-DFO-B aqueous complexes (Figure 4(a)).

3.4. aHA Sorption on CPY and Mechanism of Dissolution. The sorption behavior of aHA as a function of time and input aHA concentration is shown in Figure 6. aHA sorption envelope on CPY particles is shown in Figure 6(a). aHA sorption on CPY is pH independent between pHs 3.5 and 8.0 but increases sharply at pH 9 and further increases at pH 9.5 (Figure 6(a)). The PZC of CPY is 6.7 and IEP of aHA is 9 [19] indicating that, between pH 3.5 and ~6.5, both CPY and aHA are positively charged. Between pHs 6.5 and 9, CPY carries a small negative charge while aHA continues to be positively charged. If aHA sorption on CPY is electrostatically controlled, we would observe maximum aHA sorption between pHs 6.5 and 9. However, no pH dependence on aHA sorption is observed between pHs 3.5 and 8. The amount of aHA sorbed on CPY increases dramatically beyond pH 8 (Figure 6(a)) where CPY is negatively charged and aHA is neutral or carries a small negative charge. These results suggest the influence of hydrogen bonding in addition to the electrostatic forces in aHA sorption on CPY. The kinetics of aHA sorption were rapid with maximum sorption occurring at 1 h and staying constant at 6 h (Figure 6(b)). The rapid kinetics of aHA sorption explain rapid dissolution kinetics of CPY. Beyond 6 h, the concentration of adsorbed aHA with time varied erratically and reduced with increasing time suggesting that the sorption mechanism was complex (Figure 6(b)). aHA sorption isotherm on CPY at pH 6.5 exhibited a typical ligand-like behavior until 20 h (Figure 6(c)). The concentration of adsorbed aHA slightly reduced at 48 h. The maximum aHA sorption density on CPY was ~14 μmol/g comparable to its sorption density of 10 μmol/g on goethite (Figure 6(c)).

Since aHA sorbs at all pHs, we expect aHA sorption to affect CPY dissolution at all pHs. If concentration of aHA sorbed on CPY is the only factor affecting CPY dissolution then one would expect maximum aHA promoted CPY dissolution at pH 9. This is indeed true from our experimental results of aHA promoted CPY dissolution (Figures 4(a) and 6(a)). In addition, rapid sorption kinetics suggest that formation of the ligand surface complex is likely not the rate limiting step in CPY dissolution. Unlike goethite where

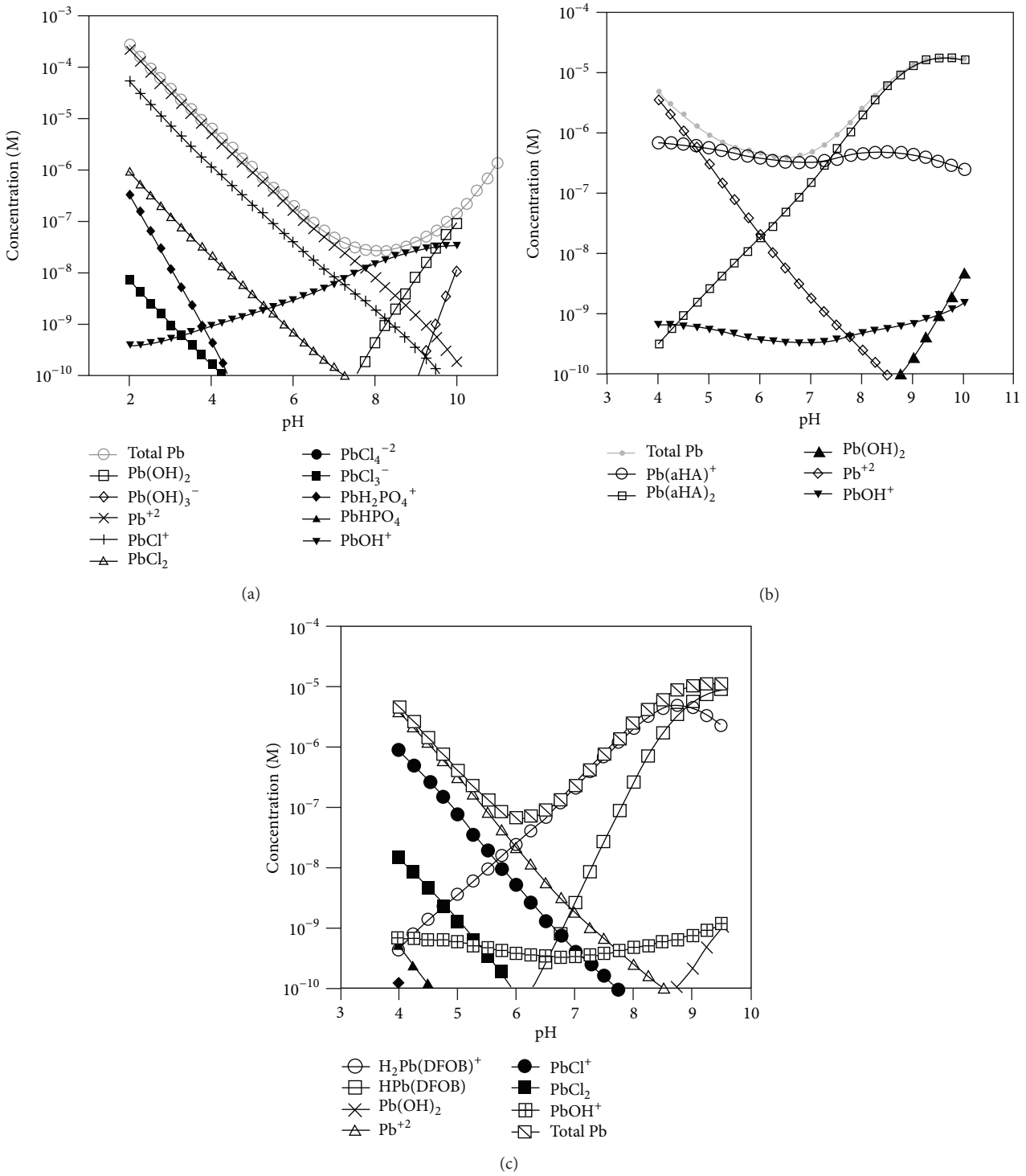

Figure 5: Visual Minteqa 2 model calculations of aqueous Pb speciation: (a) in the absence of ligands, (b) in the presence of aHA, and (c) in the presence of DFO-B.

"A" type surface hydroxyls (Fe-OH) interact with aHA [8], the surface structure of CPY is more complex containing not only Pb hydroxyl groups but also orthophosphate surface functional groups [20] that can interact with aHA or DFO-D_1. Similar to aHA, we expect DFO-D_1 sorption density of CPY to affect its efficacy in releasing lead. Unlike DFO-B that carries a positive charge at pH < 9, DFO-D_1 is uncharged [7, 11]. Lead complexation with DFO-B in solution using extended X-ray absorption fine structure spectroscopy showed formation of Pb-DFO-B hexadentate complexes at pHs of 7.5 to 9.0 and bidentate and tetradentate complexes at pH < 7.5 [21]. The inherent flexibility of DFO-B and DFO-D_1

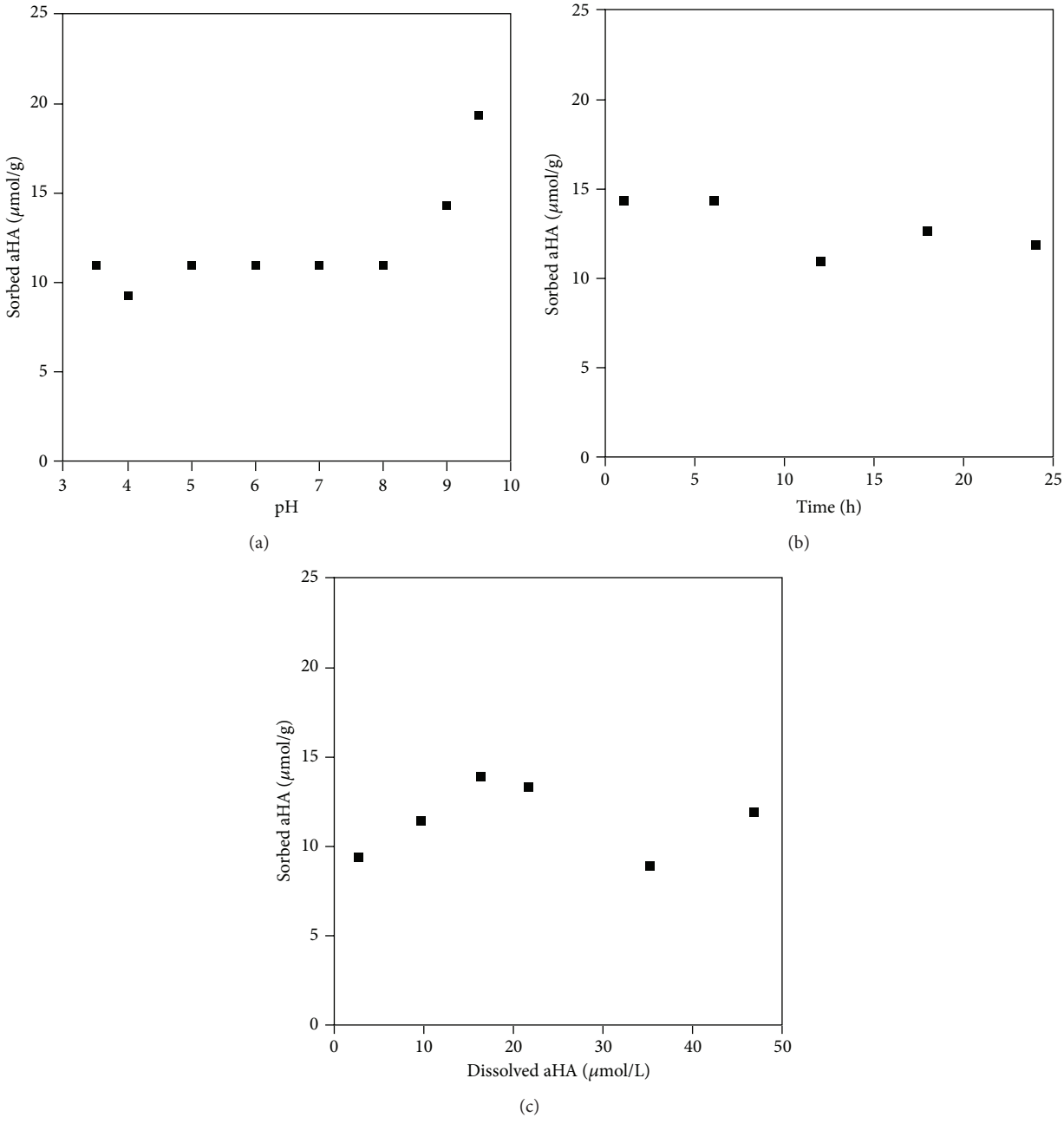

Figure 6: (a) Sorption envelope of aHA on CPY with replications at pHs 4, 7, and 9; (b) kinetics of aHA sorption on CPY at pH 6.5 with replications at 6 h and 24 h; (c) sorption isotherm of aHA sorbed on CPY at pH 6.5 with replication at 35 μmol/L. The replicates showed essentially identical sorption numbers.

due to the presence of two alkane chains between each hydroxamate moiety suggests that conformations similar to those in solution complexes may also be possible at the surface except that the positively charged DFO-B will be repelled at pH < PZC of CPY at 6.7. The expected maximum DFO-D_1 promoted Pb dissolution at pH > 7 is therefore consistent with the experimental results (Figure 4(a)). In addition, formation of bidentate or tridentate DFO-D_1 complexes involving two or three Pb-OH surface groups on CPY could potentially explain much greater dissolution rates and Pb(II) release as promoted by DFO-D_1 than aHA (Figure 4(a)).

3.5. Implications for CPY Stability in Soils and Sediments. Results on DFO-D_1 and aHA promoted dissolution of CPY here under controlled conditions are representative of many soils and sediments. These results showing significant enhancement in CPY lability due to ligand-promoted dissolution suggest that CPY formation in soils under addition of dissolved phosphate and phosphate mineral amendments will be stable at acid conditions but not at alkaline conditions. This not only is indeed consistent with results of Stanforth and Qui [22] and Cao et al. [23] in soils pertaining to Pb immobilization as CPY but also explains them. Stanforth and

Qui [22] treated lead contaminated soil waste with phosphate based additives and found a reduction in lead solubility in the acid pH range but not in the alkaline pH range. Similarly, Cao et al. [23] showed that, in lead contaminated soil and soils spiked with various Pb-based minerals such as cerrusite ($PbCO_3$), litharge (PbO), and anglesite ($PbSO_4$) and treated with $Ca(H_2PO_4)_2$ P amendment transformed Pb to pyromorphite effectively at acid pH. As noted above, lead remediation in soils as CPY is contingent on its stability which is mainly affected by commonly present ligands such as siderophores. Therefore, siderophores (DFO-D_1 and DFO-B) enhancing CPY dissolution only at alkaline pH (see Figure 4(a)) explain the efficacy of Pb remediation in soils at only acid pH as observed by Stanforth and Qui [22] and Cao et al. [23].

4. Conclusions

The trends in kinetics and equilibrium ligand-promoted dissolution of CPY can be explained by its ligand sorption behavior. All the results combined, especially the pH-dependent ligand-promoted dissolution of CPY, indicate that hydroxamate ligands can dramatically increase CPY lability in alkaline environments. In addition, uncharged trihydroxamate siderophores are more effective in dissolving Pb than positively charged trihydroxamate siderophores such as DFO-B or monohydroxamate moieties such as aHA.

Abbreviations

CPY: Chloropyromorphite
aHA: Acetohydroxamic acid
DFO-B: Desferrioxamine-B
DFO-D_1: Desferrioxamine-D_1.

Conflict of Interests

The author declares that there is no conflict of interests regarding the publication of this paper.

Acknowledgments

The author thanks Jennifer Forsythe for her help with SEM/EDS and BET surface area analysis and Dr. Patricia Maurice for providing overall support and helpful suggestions for conducting this work. Funding for this research was provided by the Center of Environmental Science and Technology at University of Notre Dame.

References

[1] G. M. Hettiarachchi and G. M. Pierzynski, "Soil lead bioavailability and in situ remediation of lead-contaminated soils: a review," *Environmental Progress*, vol. 23, no. 1, pp. 78–93, 2004.

[2] J. A. Ryan, K. G. Scheckel, W. R. Berti et al., "Reducing children's risk from lead in soil," *Environmental Science and Technology*, vol. 38, no. 1, pp. 18A–24A, 2004.

[3] K. G. Scheckel and J. A. Ryan, "Effects of aging and pH on dissolution kinetics and stability of chloropyromorphite," *Environmental Science & Technology*, vol. 36, no. 10, pp. 2198–2204, 2002.

[4] P. E. Powell, P. J. Szaniszlo, G. R. Cline, and C. P. P. Reid, "Hydroxamate siderophores in the iron nutrition of plants," *Journal of Plant Nutrition*, vol. 5, pp. 653–673, 1982.

[5] D. E. Crowley and D. Gries, "Modeling of iron availability in the plant rhizosphere," in *Biochemistry of Metal Micronutrients in the Rhizosphere*, J. A. Manthey, D. E. Crowley, and D. G. Luster, Eds., pp. 199–223, CRC Press, Boca Raton, Fla, USA, 1994.

[6] B. J. Hernlem, L. M. Vane, and G. D. Sayles, "Stability constants for complexes of the siderophore desferrioxamine B with selected heavy metal cations," *Inorganica Chimica Acta*, vol. 244, no. 2, pp. 179–184, 1996.

[7] S. M. Kraemer, S. F. Cheah, R. Zapf, J. Xu, K. N. Raymond, and G. Sposito, "Effect of hydroxamate siderophores on Fe release and Pb(II) adsorption by goethite," *Geochimica et Cosmochimica Acta*, vol. 63, no. 19-20, pp. 3003–3008, 1999.

[8] B. A. Holmén and W. H. Casey, "Hydroxamate ligands, surface chemistry, and the mechanism of ligand-promoted dissolution of goethite [α-FeOOH(s)]," *Geochimica et Cosmochimica Acta*, vol. 60, no. 22, pp. 4403–4416, 1996.

[9] L. Xie and D. E. Giammar, "Equilibrium solubility and dissolution rate of the lead phosphate chloropyromorphite," *Environmental Science & Technology*, vol. 41, no. 23, pp. 8050–8055, 2007.

[10] M. Manecki and P. A. Maurice, "Siderophore promoted dissolution of pyromorphite," *Soil Science*, vol. 173, no. 12, pp. 821–830, 2008.

[11] D. C. Edwards and S. C. B. Myneni, "Hard and soft X-ray absorption spectroscopic investigation of aqueous Fe(III)-hydroxamate siderophore complexes," *Journal of Physical Chemistry A*, vol. 109, no. 45, pp. 10249–10256, 2005.

[12] M. Manecki, P. A. Maurice, and S. J. Traina, "Uptake of aqueous Pb by Cl^-, F^-, and OH^- apatites: mineralogic evidence for nucleation mechanisms," *American Mineralogist*, vol. 85, no. 7-8, pp. 932–942, 2000.

[13] F. Bergmann and R. Segal, "The separation and determination of microquantities of lower aliphatic acids, including fluoroacetic acid," *The Biochemical Journal*, vol. 62, no. 4, pp. 542–546, 1956.

[14] A. H. Gillam, A. G. Lewis, and R. J. Andersen, "Quantitative determination of hydroxamic acids," *Analytical Chemistry*, vol. 53, no. 6, pp. 841–844, 1981.

[15] S. E. Hepinstall, B. F. Turner, and P. A. Maurice, "Effects of siderophores on Pb and Cd adsorption to kaolinite," *Clays and Clay Minerals*, vol. 53, no. 6, pp. 557–563, 2005.

[16] G. Furrer and W. Stumm, "The coordination chemistry of weathering: I. Dissolution kinetics of δ-Al_2O_3 and BeO," *Geochimica et Cosmochimica Acta*, vol. 50, no. 9, pp. 1847–1860, 1986.

[17] C. Amrhein and D. L. Suarez, "The use of a surface complexation model to describe the kinetics of ligand-promoted dissolution of anorthite," *Geochimica et Cosmochimica Acta*, vol. 52, no. 12, pp. 2785–2793, 1988.

[18] C. Ludwig, W. H. Casey, and P. A. Rock, "Prediction of ligand-promoted dissolution rates from the reactivities of aqueous complexes," *Nature*, vol. 375, no. 6526, pp. 44–47, 1995.

[19] M. T. Caudle, C. D. Caldwell, and A. L. Crumbliss, "Dihydroxamic acid complexes of iron (III): ligand pKa and coordinated water hydrolysis constants," *Inorganica Chimica Acta*, vol. 240, no. 1-2, pp. 519–525, 1995.

[20] Å. Bengtsson, A. Shchukarev, P. Persson, and S. Sjöberg, "A solubility and surface complexation study of a non-stoichiometric hydroxyapatite," *Geochimica et Cosmochimica Acta*, vol. 73, no. 2, pp. 257–267, 2009.

[21] B. Mishra, E. A. Haack, P. A. Maurice, and B. A. Bunker, "Effects of the microbial siderophore DFO-B on Pb and Cd speciation in aqueous solution," *Environmental Science and Technology*, vol. 43, no. 1, pp. 94–100, 2009.

[22] R. Stanforth and J. Qiu, "Effect of phosphate treatment on the solubility of lead in contaminated soil," *Environmental Geology*, vol. 41, no. 1-2, pp. 1–10, 2001.

[23] X. Cao, L. Q. Ma, S. P. Singh, and Q. Zhou, "Phosphate-induced lead immobilization from different lead minerals in soils under varying pH conditions," *Environmental Pollution*, vol. 152, no. 1, pp. 184–192, 2008.